

CHAPTER 4: FAST BEAM-FOIL EXPERIMENT 36

4.1 THE BEAM-FOIL LIGHT SOURCE 36
 4.2 EXCITATION MECHANISMS..... 38
 4.3 SPECTROMETERS AND DETECTORS..... 46
 4.4 TARGETS 51
 4.5 EXPERIMENTAL METHOD 51
 4.6 EXPERIMENTAL PROBLEMS 54

FIG. 4.1 THE PRINCIPLE OF FAST BEAM-FOIL SPECTROSCOPY. IONS FROM THE ACCELERATOR ARE MASS-ANALYZED AND SENT THROUGH A THIN FOIL. THE RADIATION EMITTED ON THE DOWNSTREAM IS STUDIED BY OPTICAL, X-RAY, OR ELECTRON SPECTROSCOPY. LIFETIME AND QUANTUM BEAT EXPERIMENTS ARE ALSO INDICATED. 36

FIG. 4.2. SCALING OF ION ENERGY CHANGE WITH REDUCED ION VELOCITY ($V/Z^{2/3}$). BOHR AND OTHERS SUGGESTED THAT THE CHARGE STATES OF AN ION COULD BE ESTIMATED BY ASSUMING THAT IT WOULD LOSE ALL OF ITS ELECTRONS WHOSE ORBITAL VELOCITY WAS LESS THAN THE ION VELOCITY. THE ORBITAL VELOCITY OF ELECTRON WAS CONSIDERED TO BE PROPORTIONAL TO $Z^{2/3}$, SO THIS CONCEPT CAN BE ILLUSTRATED BY PLOTTING STOPPING VS AN ION VELOCITY REDUCED BY THIS ELECTRON VELOCITY FACTOR..... 41

FIG. 4.2. SCALING OF ION ENERGY CHANGE WITH REDUCED ION VELOCITY [$V/(V_F Z^{2/3})$]. BOHR ESTIMATED THE CHARGE STATE OF AN ION BY ASSUMING THAT IT WAS STRIPPED OF ANY OF ITS ELECTRONS WHOSE ORBITAL VELOCITY WAS LESS THAN ITS VELOCITY SEE FIG. 4.2. THIS CONCEPT LASTED FOR THIRTY YEARS BECAUSE OF ITS ELEGANT SIMPLICITY. BRANDT EXTENDED THIS IDEA TO RELATE THE ION VELOCITY AND ITS ELECTRONS TO THE ELECTRON VELOCITY OF THE FOIL, IN WHICH IT IS PASSING. ZIEGLER TOOK THIS CONCEPT AND MADE AN EXPLICIT FORMULATION THAT REDUCED THE ION VELOCITY COULD TAKE THE FORM OF $V/(V_F Z^{2/3})$ 41

FIG. 4.4. THE OPTIMAL ION BEAM ENERGY OF THE IONIZATION DEGREES WITH THE EFFECTIVE CHARGE $Z^* = (Z-\Sigma)$ AND MOST ABUNDANT ISOTOPE OF ATOMIC WEIGHT A LISTED IN TABLE 4.1. 43

FIG. 4.5. EQUILIBRIUM CHARGE DISTRIBUTION OF: (A) CARBON, (B) NITROGEN, (C) OXYGEN, AND (D) NEON AS A FUNCTION OF INCIDENT ION. FROM THE ABOVE WE CAN FIND THE OPTIMAL ENERGY TO GET THE IONS NEEDED IN THE EXPERIMENTS. FOR OXYGEN WE NEEDED TO STUDY THE HIGHER LYING SEXTET STATES IN O IV (O^{3+}). IN (C) WE COULD SEE THAT 2-3 MeV IS A POSSIBLE OPTIMAL ENERGY [82]. 44

FIG. 4.6. THE 1-M SEYA-NAMIOKA TYPE CONCAVE GRATING MONOCHROMATOR AT LIÈGE. THE DISTANCES $L_A = L_B = 1$ METER AND THE ANGLE $\Phi=70.25$ DEGREES ARE FIXED. IN ORDER TO SCAN WAVELENGTHS, THE GRATING IS ROTATED ABOUT ITS 47
 VERTICAL AXIS. FOR THE MAXIMUM EFFICIENCY A AND B ARE ON THE ROWLAND CIRCLE..... 47

FIG. 4.7 THE ELECTRONICS AND DATA-TAKING EQUIPMENT IN BFS EXPERIMENTS AT THE UNIVERSITY OF LIÈGE. 51

FIG. 4.8. THE EXPERIMENTAL SETUP OF FAST BEAM-FOIL SPECTROSCOPY ON A 2 MeV VAN DE GRAAFF ACCELERATOR BEAM LINE AT THE UNIVERSITY OF LIÈGE [14,106]. 52

FIG. 4.9. THE BEAM-FOIL INTERACTION IN THE VACUUM CHAMBER WORKS AS AN EFFICIENT LIGHT SOURCE IN THE BEAM-FOIL SPECTROSCOPY AT THE UNIVERSITY OF LIÈGE. 53

TABLE 4.1 THE OPTIMAL ION BEAM ENERGIES (IN MeV) OF THE IONIZATION DEGREES WITH THE EFFECTIVE ION CHARGE $Z^* = (Z-\Sigma)$, Σ IS ELECTRONIC SCREENING OF THE BEAM ION AFTER COLLISION WITH FOIL ATOM, AND MOST ABUNDANT ISOTAPE OF ATOMIC WEIGHT A, BY THIS WORK. 42

TABLE 4.2 COMPARISONS OF THE CALCULATED OPTIMAL BEAM ION ENERGIES (IN MeV) BY THIS WORK WITH EXPERIMENTAL DATA (IN MeV) FROM [82]. 45

CHAPTER 4

FAST BEAM-FOIL EXPERIMENT

4.1 The Beam-Foil Light Source

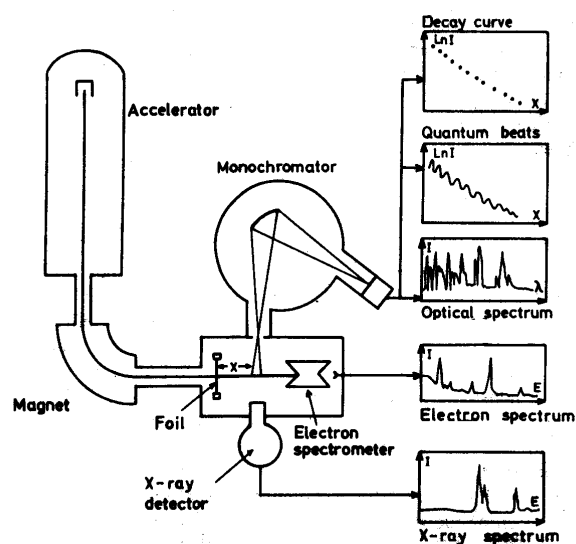


FIG. 4.1. The principle of fast beam-foil spectroscopy. Ions from the accelerator are mass-analyzed and sent through a thin foil. The radiation emitted on the downstream is studied by optical, x-ray, or electron spectroscopy. Lifetime and quantum beat experiments are also indicated. [The figure is from [19].]

The principle of fast beam-foil spectroscopy is illustrated in Fig. 4.1. An ion accelerator produces a beam of fast ions which are magnetically analyzed to ensure a chemically and isotopically pure beam and then directed through a thin (typically $10 \mu\text{g}/\text{cm}^2$ thickness) exciter foil, usually made of carbon. Because of collisions with the foil atoms, the fast ions may undergo further ionization

(electron capture is also possible at lower ion velocity), and they often exit the foil in excited electronic and atomic states. These ions decay on the downstream side of the foil through the emission of light in the ultraviolet, visible or soft x-ray regions. As schematically shown in Fig. 4.1 electron emission also occurs.

The foil excited ion beam can be considered as a light source for atomic spectroscopy in a wide sense (i.e., including electron spectroscopy). There are several interesting and quite attractive properties that characterize this spectroscopic source. It has wide applicability. Practically all elements can be accelerated in modern ion accelerators. More than 70 different chemical elements have already been studied by the beam-foil technique. By varying the accelerator energy it is possible to reach many ionization degrees (see chapter 4.2). The presently available beam-foil spectroscopic results include neutrals as well as more than 40 times ionized atoms. The excitation is largely unselective, which means that very many levels in any ion of interest can be studied. This broad-band excitation also has drawbacks (see chapter 4.6). The acceleration to a well-defined energy and subsequent magnetic analysis usually guarantees a chemically and isotopically pure beam, and the beam-foil spectroscopy light source is therefore free from impurities that are present in other spectroscopic light sources. One exception is that certain transitions in atomic carbon, excited foil atoms from sputtered, are observed [39]. The other possible exception is that other beams with the same mass/charge ratio M/Q are not resolved magnetically. The rest gas pressure in the target chamber is typically 10^{-6} torr (or lower) and the decay of the excited states of the fast ions are therefore not influenced by secondary collisions and excitations. Additional and more detailed information can be found in the following sections and many references [7-12].

4.2 Excitation Mechanisms

The ion-foil or ion-gas interaction is a convenient way of exciting the atomic states. In this section, we present briefly the understandings and the results about the excitation itself.

The excitation of ion beam in a foil target is basically the study of screened Coulomb collisions between two colliding atoms. In the 1950's, major advances were made in studies of the energy loss of the ion to target nuclei. Bohr summarized much of the earlier work in 1948 [40] that using the Thomas Fermi model to estimate the screened Coulomb potential, $V(r)$ between atoms:

$$V(r) = (Z Z_1 e^2 / r) \exp (-r / a), \quad (4.4.1)$$

where Z and Z_1 are the atomic numbers of an ion and an target atom, r is their separation, and a is a "screening parameter". Bohr argued that a reasonable approximation might be [40]:

$$a = a_0 / (Z^{2/3} + Z_1^{2/3})^{1/2}, \quad (4.4.2)$$

where a_0 is the Bohr radius, but this approximation was not derived.

Firsov took a more practical approach and used numerical techniques to derive the interatomic potentials of two colliding Thomas-Fermi atoms [41,42]. After finding the numeric values of the potentials as a function of the atomic separation he then fitted these potentials using the Thomas-Fermi screening length and found that the best fit was obtained with:

$$a = a_0 / (Z^{1/3} + Z_1^{1/3})^{2/3}. \quad (4.4.3)$$

For the degree of ionization of the ion as it goes through materials, Bohr suggested [43,44] that the ion be considered to be stripped of all electrons with velocities lower than the ion velocity. Bohr and others suggested that one simple

criterion would be to assume that ions lose electrons whose orbital velocities v_o would be less than the ion velocity v . Using the Thomas Fermi atom he could show that the ion charge *fraction*, Z^* / Z , would be :

$$Z^* = Z^{1/3} v / v_o, \quad (4.4.4)$$

where Z is the atomic number of the ion, and Z^* is its effective charge of the electron in the ion after collision with energy loss to the target electrons, v is the ion velocity and v_o is the Bohr velocity ($\sim 2 \times 10^8$ cm/sec) which is the approximate velocity of the electron in an electronic orbit in ion. It is called Bohr criterion. Lamb [45] considered the same problem as Bohr, and suggested a similar effective charge approximation, but based on the energy rather than the velocity of the ion's electrons. Lamb also got a similar, but less detailed, expression for energy change assuming Thomas-Fermi atoms.

In perturbation theory this ratio should scale as $(Z^*)^2$ where Z^* is the number of electrons left on the ion. He found a large amount of data could be accurately described using the relation:

$$Z^* / Z = 1 - a \exp\left(\frac{b}{Z^{2/3}} \cdot \frac{v}{v_o}\right), \quad (4.4.5)$$

where a and b are fitting constants. The expression expands to be the Bohr relationship (assuming $a = b = 1$).

In 1963 the first unified approach to energy change and range theory was made by Lindhard, Scharff and Schiott [46-47] and their approach is commonly called the LSS-theory. With this theory it was possible to predict the range of ions in solids within a factor of two - a remarkable achievement considering it was applicable over the entire range of atomic species and energies up to the energy change maximum [48-59]. Since it was based on Thomas-Fermi atoms it

was most accurate for atoms with many electrons in the intermediate range where they are neither fully stripped nor almost neutral. The theory naturally shows no shell effects.

The LSS theory was the last of the comprehensive theories based on statistical models of atom-atom collisions. Improvements in calculating energy change and ranges over the next twenty years were made by using numerical techniques and removing some of the approximations used by Bohr, Firsov and Lindhard. One new theoretical insight that has had profound implications was made by Brandt and Kitagawa where they revised the Bohr suggestion of the degree of ionization of ions traveling within solids. Bohr had suggested that the ion's electrons that had orbital velocities less than the instantaneous velocity of the ion would be stripped off, leaving the ion only with its inner high-velocity electrons. Brandt and Kitagawa suggested that this stripping criteria should be modified to consider the ion's electron velocity only relative to the Fermi velocity of the solid. They then proceeded to develop the formalism to allow the full evaluation of this new concept that has proved to be quite accurate. The two concepts are illustrated in Figs. 4.2 and 4.3.

Energy changes in 2003 (the date of this chapter) can now be calculated with an average accuracy of about 5% overall, 6% for heavy ions and better than 2% for high velocity light ions. Range distributions for amorphous elemental targets have about the same accuracy.

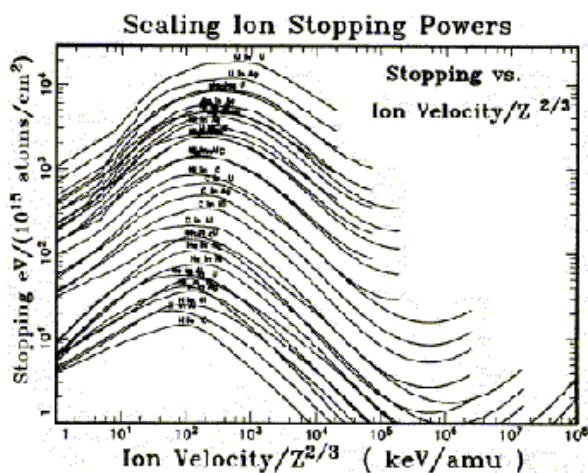


FIG. 4.2. Scaling of ion energy change with reduced ion velocity ($V/Z^{2/3}$). Bohr and others suggested that the charge states of an ion could be estimated by assuming that it would lose all of its electrons whose orbital velocity was less than the ion velocity. The orbital velocity of electron was considered to be proportional to $Z^{2/3}$, so this concept can be illustrated by plotting stopping vs an ion velocity reduced by this electron velocity factor. [The figure is from [57].]

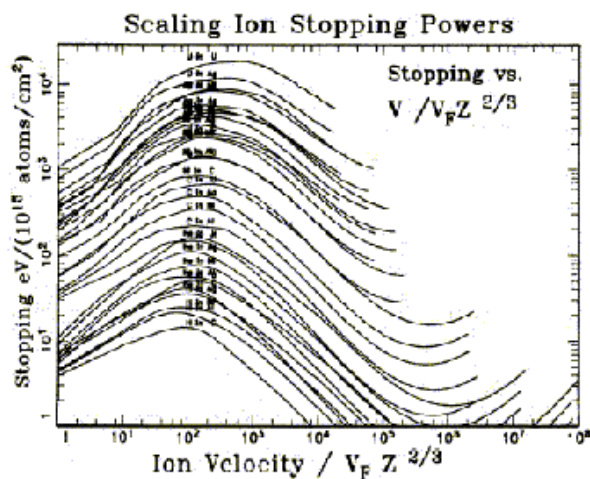


FIG. 4.3. Scaling of ion energy change with reduced ion velocity [$V/(V_F Z^{2/3})$]. Bohr estimated the charge state of an ion by assuming that it was stripped of any of its electrons whose orbital velocity was less than its velocity see Fig. 4.2. This concept lasted for thirty years because of its elegant simplicity. Brandt extended this idea to relate the ion velocity and its electrons to the electron velocity of the foil, in which it is passing. Ziegler took this concept and made an explicit formulation that reduced the ion velocity could take the form of $V/(V_F Z^{2/3})$. [The figure is from [57].]

Relevant reviews are made by Whaling , Fano [60], Jackson [61,62], Bichsel [63], Sigmund [64], Ahlen [65], Ziegler, *et al.* [66-70], and the International Commission on Radiation Units and Measurements [71.72]. For original sources, the theoretical treatment of the energy change of ions in matter is due greatly to the work of Bohr [40,73,74], Bethe [75-77], Bloch [78-79], Firsov [41-42,80-81] and Lindhard [47-51].

From Fig. 4.2 and Fig. 4.3 we could see that theoretical energy changes are quite similar with the Bohr criterion and the modified Bohr criterion. For the simplicity, in this work we used the Bohr criterion to estimate the optimal energy we needed in the beam-foil experiments.

Using the Bohr criterion (4.4.4), we obtained the optimal ion beam energies for the ionization stages for the possible observations of sextet states in doubly excited O IV, F V and Ne VI. The results are shown in Table 4.1 and Fig. 4.4.

TABLE 4.1. The optimal ion beam energies (in MeV) of the ionization degrees with the effective ion charge $Z^ = (Z-\sigma)$, σ is electronic screening of the beam ion after collision with foil atom, and most abundant isotope of atomic weight A , by this work.*

Z	A	$\sigma=4$	$\sigma=3$	$\sigma=2$	$\sigma=1$	$\sigma=0$
6	12	0.3	0.7	1.2	1.9	2.7
7	14	0.7	1.3	2.0	2.9	3.9
8	16	1.3	2.1	3.0	4.1	5.3
9	19	2.3	3.3	4.5	5.9	7.4
10	20	3.2	4.4	5.7	7.3	9.0
11	23	4.7	6.2	7.8	9.7	11.7
12	24	6.1	7.7	9.5	11.5	13.7

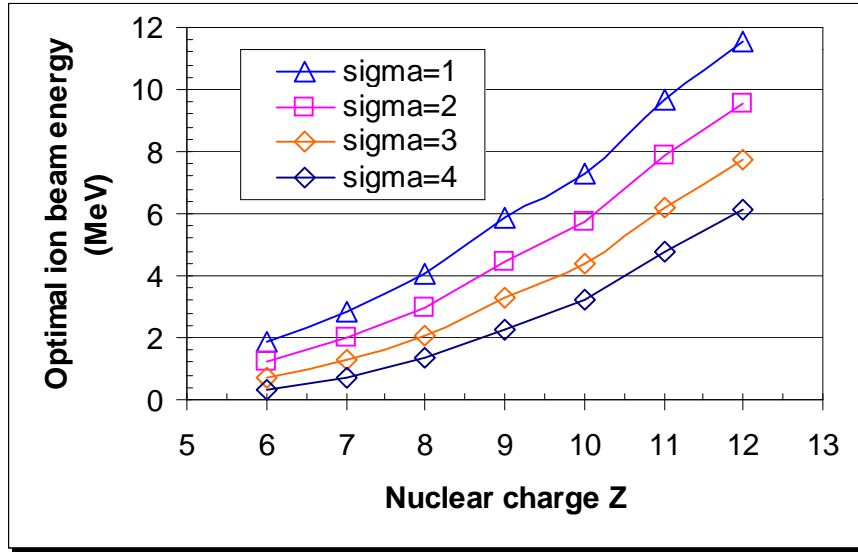


FIG. 4.4. The optimal ion beam energy of the ionization degrees with the effective charge $Z^* = (Z-\sigma)$ and most abundant isotope of atomic weight A listed in Table 4.1.

As shown in Fig. 2.1, the energies of the sextet levels of O IV have very high energies, due principally to the 1s and 2s electron vacancies. These 5-electron high-spin states have energies typically just below the 2-electron O VII 1s2s and 1s2p states, about 0.8 keV above the O IV ground state. It is reasonable to assume that the beam ion energies for $\sigma \sim 2$ are optimal for the observations of the transitions between sextet states in O IV, F V and Ne VI. These energies are about 3.0 MeV, 4.5 MeV and 5.7 MeV, respectively.

The experimental charge distributions that were helpful for our experiments were found in [82] and are shown in Fig. 4.5. Using the modified Bohr criterion, Stelson [83] has calculated the ionization degrees that can be reached with high-energy machines. The energies, required to ionize O IV, F V and Ne VI in order to create vacancies in the K and L shells, are found to be about 0.2 MeV/amu and 0.1 MeV/amu, respectively. Using Fig 4.5 we could see that 2.5 MeV and 5

MeV are approximately the optimal beam ion energies for the observations of the transitions between sextet states in O IV and Ne VI. They are close to the calculated values of 3.0 MeV and 5.7 MeV.

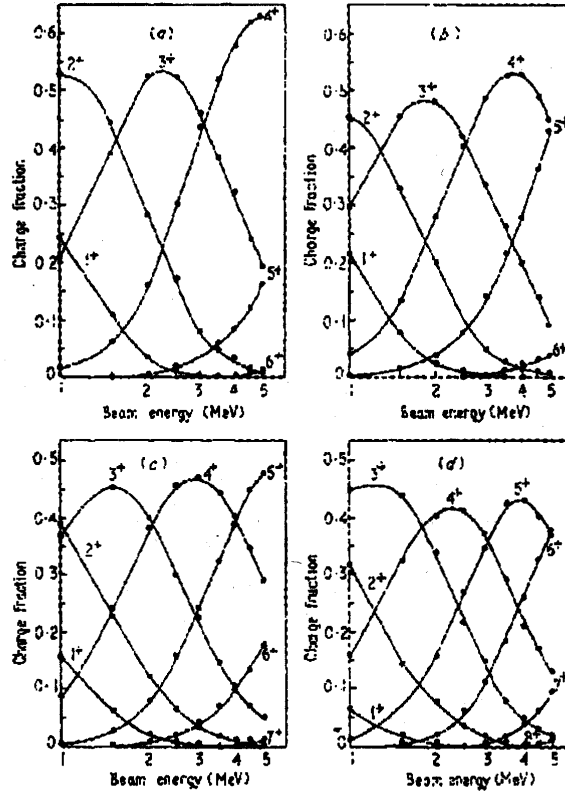


FIG. 4.5. Equilibrium charge distribution of: (a) carbon, (b) nitrogen, (c) oxygen, and (d) neon as a function of incident ion. From the above we can find the optimal energy to get the ions needed in the experiments. For oxygen we needed to study the higher lying sextet states in O IV (O^{3+}). In (c) we could see that 2-3 MeV is a possible optimal energy. [The figure is from [82].]

The comparisons of the calculated optimal beam ion energies by this work with experimental data from [82] are indicated in Table 4.2. Here we set the electronic screenings σ assuming that the screened Coulomb field at the position

of the valence electron in the most outer shell is screened completely by all other electrons: i. e. there is no penetration into the orbits of other electrons. The accuracy of the calculations is within 65 %. It is clear that, with the Bohr criterion approach, most energy changes can be estimated to better than a factor of two.

TABLE 4.2. Comparisons of the calculated optimal beam ion energies (in MeV) by this work with experimental data (in MeV) from [82].

	σ	Ecal	Eexp	accuracy
C ⁴⁺	1	1.9	5.0	62 %
C ³⁺	2	1.2	2.0	40 %
C ²⁺	3	0.7	1.0	30 %
N ⁴⁺	2	2.0	3.3	39 %
N ³⁺	3	1.5	1.3	13 %
O ⁴⁺	3	2.5	2.1	16 %
O ³⁺	4	1.4	1.3	7 %
Ne ⁴⁺	4	3.4	3.2	6 %

From ion-atom collision theory the populations in the levels (nl) are expected to be proportional to $[(2l+1) n^{-q}]$ with $q \sim 3$. Support for this model has been found in several experiments. For example, Davison [84], Dynefors *et al.* [85], and Heine *et al.* [86] found that the n^{-3} dependence agreed with experimental data. However, other values of q have also been proposed. Thus, Curtis [87] noted that certain decay curves for highly ionized levels of higher angular momentum showed such pronounced cascading tails that $q=1-2$ must be assumed. However, such distributions diverge unless they are truncated for certain n values. The studies [88-89] show that the n^{-q} , $q \sim 3$ dependence is at best

highly approximate. Certain n states may be preferentially populated as the result of near-resonant charge transfer between the fast ions and foil atoms.

The dependence for a given n has been extensively investigated. Work [90] indicates that here s states are overpopulated in comparison to p states, whereas for higher angular momentum the statistical $2l+1$ dependence seems to be approximately valid. Indeed even more pronounced populations of high l states have been noted [91]. Heine *et al.* [86] also found that the l dependence varies with the energy. Other data show irregularities in l populations [92]. A model based on information theory has been applied to beam-foil excitations by Aberg and Goscinski [93]. The n^{-3} dependence has been shown for large n and a given l . The dependence of beam energy is being investigated. Such calculations are expected to give much new insight into the excitation processes.

4.3 Spectrometers and Detectors

The particle density in the beam-foil light source is typically $10^5/\text{cm}^3$, which is several orders of magnitude lower than in most other spectroscopic light sources. Relatively fast optical equipment (with a corresponding sacrifice of high spectral resolution) is usually needed for recording the spectra. Depending on the wavelength (energy) of the detected photons, various optical instruments are being used by BFS investigators. In the air region (wavelength $\lambda > 2000 \text{ \AA}$), relatively simple scanning grating monochromators, *e.g.*, of Czerny-Turner type, are frequently used. The focal length of the instruments range from about 0.25 m to 2.0 m. Below 2000 \AA vacuum instruments must be used. These are usually of normal-incidence or of Seya-Namioka design [94] and are appropriate for the region $300\text{-}4000 \text{ \AA}$ (40 - 3 eV). Grazing-incidence

spectrometers are needed for investigations of shorter-wavelength regions (20-500 Å). Here, also, both commercial and home-made instruments (with 1-3 m focal lengths) have been used [95-96], and the wavelengths covered range from about 20 to 600 Å (600-20 eV). All these spectrometers are usually equipped with photo-multipliers or open detectors (e.g., channeltrons) at the exit slit and pulse-counting techniques are generally being employed. In the early experiments the beam-foil spectra were frequently registered photographically [97], but nowadays the photoelectric detection methods are usually preferred, because of their linearity and higher sensitivity. Fig. 4.6 shows the 1-m Seya-Namioka spectrometer system used in this fast beam-foil experiment at Liège.

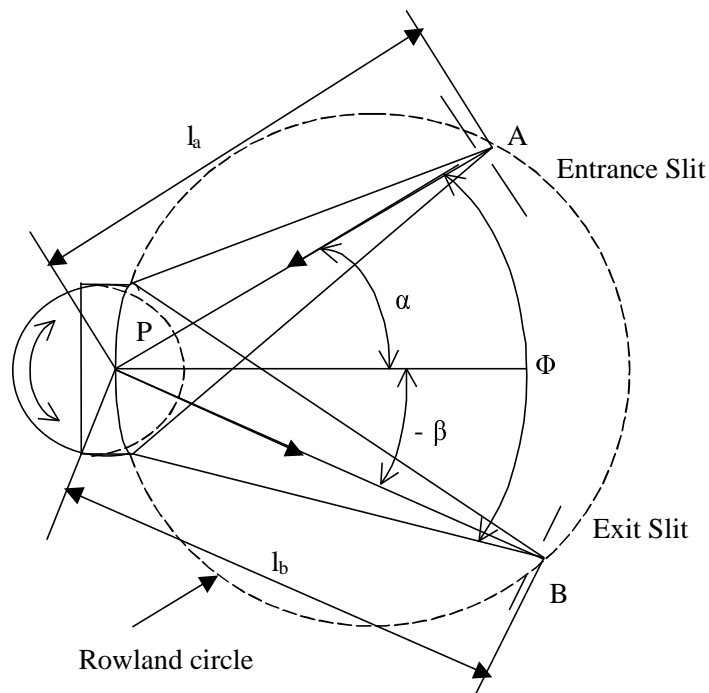


FIG. 4.6. The 1-m Seya-Namioka Type Concave Grating Monochromator at Liège. The distances $l_a = l_b = 1$ meter and the angle $\Phi = 70.25$ degrees are fixed. In order to scan wavelengths, the grating is rotated about its vertical axis. For the maximum efficiency A and B are on the Rowland circle.

The concave diffraction grating was invented in 1882 by Henry Rowland. The grating consists of finely spaced lines produced on the concave face of a spherical surface. Rowland used Fermat's principle in order to specify the precise shape and location of the grating lines. In Fig. 4.6, the beam source of the light to be diffracted is placed at Point A. The spectrum of the source for a given wavelength λ is obtained as an image at Point B. If P (x, y, z) is any point on the spherical surface, then Fermat's Principle requires that:

$$AP + BP = 2b = \text{Constant.}$$

Quoting from Rowland's original paper: "Should we increase b by equal quantities and draw the ellipsoids or hyperboloid so indicated. The intersections of these surfaces with any other surface form what are known as Huygen's zones. By actually drawing these zones on the surface we form a grating which will reflect or refract the light of a certain wavelength to the given focal point."

Thus, over a hundred years ago it was shown that an aberration-free image could be formed by a concave diffraction grating for a given wavelength, if the groove shape could be made to follow the intersection of a family of hyperbolae with the grating surface. It is well known that a hyperbolic fringe profile results from the interference pattern of two coherent point sources. The modern holographic concave aberration corrected diffraction grating is the direct result of applying laser technology with the spatial modulation capability of photoresist materials in order to "draw" the hyperbolic lines that Rowland described in the 1800's.

The modern theory of the Concave Holographic Diffraction Grating was developed by M. Seya and T. Namioka in 1954. The grating equation is

$$Nm \lambda = \sin \alpha + \sin \beta.$$

The equation of spectral plane (tangential) focus is

$$\frac{\cos^2 \alpha}{l_a} - \frac{\cos \alpha}{R} + \frac{\cos^2 \beta}{l_b} - \frac{\cos \beta}{R} - \frac{m\lambda}{\lambda_0} C_f = 0.$$

the equation of astigmatic (sagittal) focus is

$$\frac{1}{l_a} - \frac{\cos \alpha}{R} + \frac{1}{l_b} - \frac{\cos \beta}{R} - \frac{m\lambda}{\lambda_0} C_a = 0.$$

The equation of coma terms is

$$\frac{\sin \alpha}{l_a} \left(\frac{1}{l_a} - \frac{\cos \alpha}{R} \right) + \frac{\sin \beta}{l_b} \left(\frac{1}{l_b} - \frac{\cos \beta}{R} \right) - \frac{m\lambda}{\lambda_0} C_c = 0,$$

where

R = radius of curvature of spherical blank

m = the diffraction order (0, ±1, ±2, etc.)

N = 1/d is Groove frequency at center, and d is the grating period

λ₀ = wavelength used in grating fabrication

Additional higher order terms exist in the light path function. The above relations, however, are sufficient to describe the primary focal properties of the Concave Holographic Grating. A typical design approach might involve the specification of the required spectral dispersion as a function of wavelength, which establishes the groove frequency N, and the coefficient C_f. Next C_a and C_c are selected in order to minimize those remaining aberrations over the spectral range of interest. Once this constant is determined, the fabrication equations are solved simultaneously in order to establish the positions of the recording coherent point sources.

For the 1-m Seya-Namioka Type Concave Grating Monochromator used in this fast beam-foil experiment at Liège, the distances $l_a = l_b = 1$ meter and the angle $\Phi=70.25$ degrees were fixed. In order to scan wavelengths, the grating is rotated about its vertical axis. To scan the wavelength range of 300 Å to 1500 Å we used the 2400 G/mm grating, where the wavelength resolution was ~ 0.1 Å. To scan the wavelength range of 1800 Å to 3000 Å we used the 1200 G/mm grating, where the wavelength resolution was ~ 0.2 Å.

Most beam-foil experiments use single-channel methods. Multi-channel detection techniques need to be developed to reduce the time needed for data taking, particularly at large and heavily scheduled accelerators. Such detectors, for the vacuum ultraviolet region, have recently been successfully tested in beam-foil experiments [98-99].

Our BFS experiments at Liège utilized a single-channel. We show the system used at the University of Liège in Fig. 4.7. Here, the foil-excited beam (from a 1.7 MeV Van de graaff accelerator) is viewed by a monochromator, which is used for the vacuum UV region. The pulses from the photon detector at the exit slit of the monochromator were multiplied, discriminated and fed into a minicomputer. The monochromator was scanned with a stepwise rotation of the grating for a fixed amount of beam charge recorded by the digitized Faraday cup beam current counter. The minicomputer also directs the experiment by scanning the monochromator and/or moving the foil along the beam.

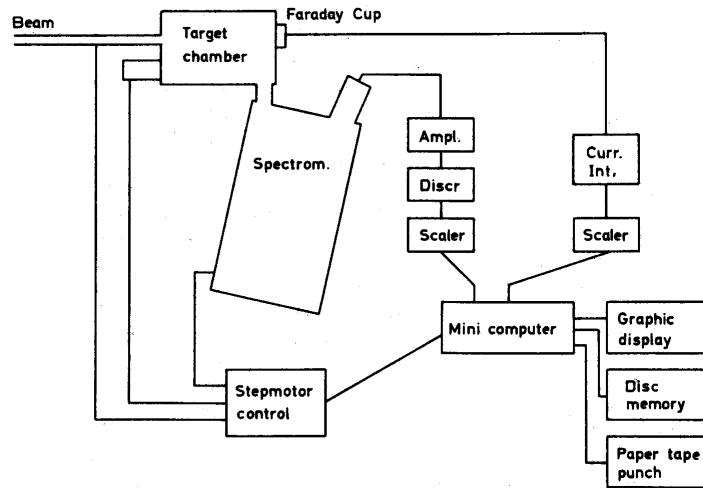


FIG. 4.7. The electronics and data-taking equipment in BFS experiments at the University of Liège.

4.4 Targets

The target foils are usually made of self-supporting carbon by evaporation [100]. Foil breakage under beam bombard is a problem in BFS experiments, particularly with beams of low-energy heavy ions. Systematic studies of such effects have been reported by several authors [101-105]. Our foils were made from a glow discharge [14] and had areal densities about $\sim 10\text{-}20 \mu\text{g}/\text{cm}^2$. They lasted for 1-2 hours under the experimental condition described below. This foil breakage posed the principal limitation on the ion beam current density and hence photon signal-to-noise ratio in our experiments.

4.5 Experimental Method

The experiments were performed with the standard fast-ion beam-foil excitation system on a 2 MeV Van de Graaff accelerator beam line at the

University of Liège [14,106]. The experimental setup of fast beam-foil spectroscopy is illustrated in Fig. 4.1. To produce the spectra of oxygen in the wavelength region near 500-1500 Å, the beam current of about 1.3 μA of $^{16}\text{O}^+$ and $^{32}\text{O}_2^+$ ions at beam energies between 1.2 and 1.7 MeV crosses a thin ($\sim 10 \mu\text{g}/\text{cm}^2$) exciter carbon foil. Light emitted at about 90 degrees to the ion beam direction was analyzed by a 1-m Seya-Namioka spectrometer equipped with a low-noise channeltron detector (see Fig. 4.8 and 4.9). 25 spectra were recorded in the wavelength range around 500-1500 Å at slit widths of 100/100 and 40/40 μm. Through the use of optical refocusing spectroscopy a full width at half maximum (FWHM) of 0.7 Å in this wavelength range was achieved.

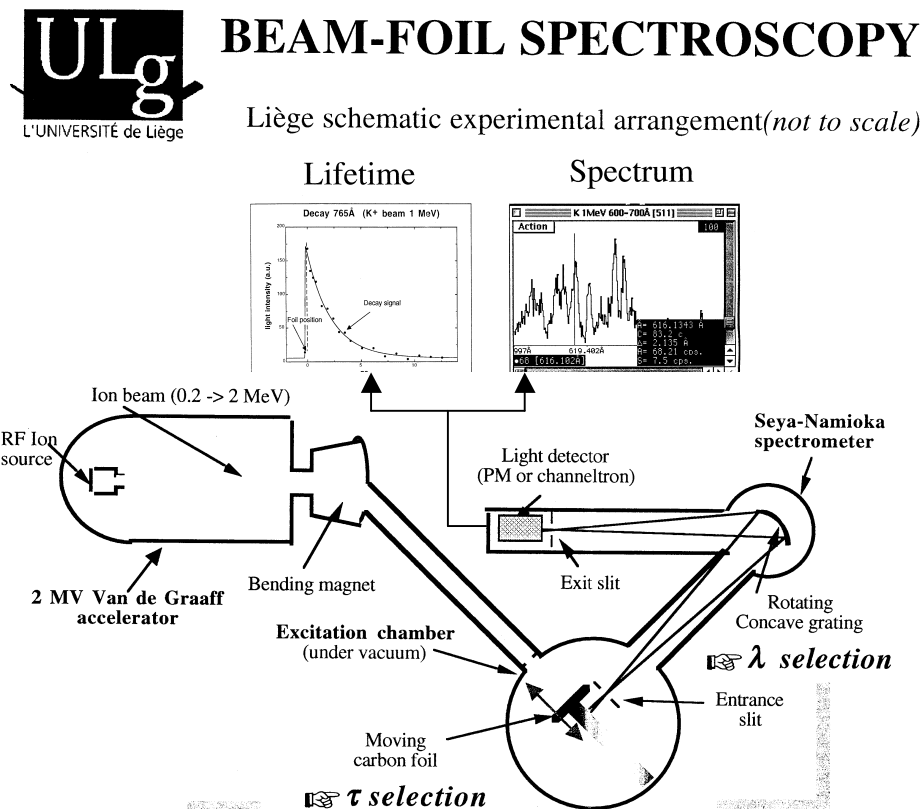


FIG. 4.8. The experimental setup of fast beam-foil spectroscopy on a 2 MeV Van de Graaff accelerator beam line at the University of Liège [14,106]. [The figure is from University of Liège.]

Beam-foil interaction chamber VUV observation

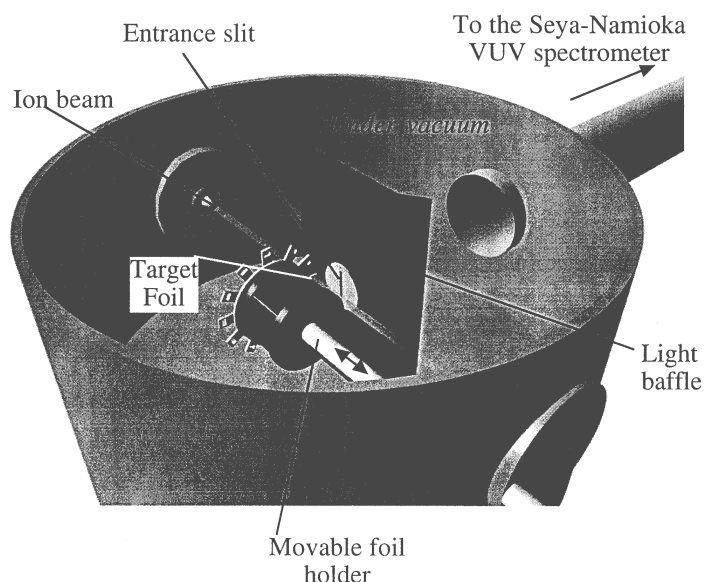


FIG. 4.9. The beam-foil interaction in the vacuum chamber works as an efficient light source in the Beam-foil Spectroscopy at the University of Liège. [The figure is from University of Liège.]

Spectra in the wavelength range where the sextet lines were expected are also available from some previous unpublished measurements in oxygen, fluorine and neon. They yield information on wavelengths, intensities and line shapes, and are very helpful for comparison with our present calculations of the sextet states and measurements in oxygen. Spectra of O^{3+} and F^{4+} were recorded from beams of $^{16}O^+$ and $^{20}(FH)^+$ ions at ion energies of 2.5 MeV with similar experimental procedures at the University of Lyon. Linewidths in the spectra range from 0.4 Å and 0.8 Å. The spectrum of neon was produced and recorded from a beam of $^{20}Ne^+$ ions at the Argonne National Lab Dynamitron Accelerator

at an energy of 4 MeV. The spectrum was taken in the 2nd grating order to help to identify and resolve the sextet spectrum. Linewidths are about 0.4 Å in the wavelength range of 490-560 Å.

4.6 Experimental Problems

Beam-foil studies of atomic spectra frequently yielded optical transitions that had not been reported in the previous literature on atomic spectroscopy. Several authors [97,107-111] thus observed new transitions in multiply ionized N and O. Only a fraction of which could be classified (i.e., assigned to definite energy levels in ionized N and O); the majority of the lines were left unidentified.

Many of the spectra of multiply ionized atoms are incompletely known. Beam-foil studies provide some new spectroscopic material. However, it was soon also realized that the beam-foil excitation populates highly excited states that are difficult to excite in other light source.

Since the line widths are of the order of 1 Å in beam-foil spectra in the UV region in the experiments, wavelengths could only be determined with ± 0.2 or ± 0.3 Å uncertainties. Occasionally, data of much better quality were also sometimes reported [112]. The line widths are largely caused by sensitivity that demands the use of small and fast monochromators and wide slits. Furthermore, the light is emitted by moving ions, and Doppler effects must be considered. When the foil-excited beam is viewed at an angle of 90 degree, the first-order Doppler shift vanishes. However, the second-order shift, proportional to v^2/c^2 , must be taken into account. The principal line widths come from Doppler broadening of the spectral lines, due to the finite acceptance angle θ of the spectrometer. The broadening is approximately given by

$$\Delta\lambda \sim \lambda \theta v/c$$

For the 1-m Seya-Namioka spectrometer of our experiment with slit widths $w = 100 \mu\text{m} / 100 \mu\text{m}$, focal length $f = 1 \text{ m}$, and a grating of $A = 10 \text{ cm}$ wide, the finite acceptance angle θ is written as

$$\theta \sim (A+w) / f$$

When we accelerate ^{16}O ions at 1.7 MeV and $v/c \sim 1.6\%$. We obtained a line broadening of $\Delta\lambda \sim 1.04 \text{ \AA}$ at the wavelength of $\lambda \sim 660 \text{ \AA}$. This clearly rules out precision spectroscopy.

Efforts have been made to reduce this drawback. When we wanted to improve the accuracy of the wavelengths, we reduced the slit widths to $w = 40 \mu\text{m} / 40 \mu\text{m}$, and used the refocusing technique. Using the two methods the line broadening was reduced to $\Delta\lambda \sim 0.8 \text{ \AA}$.

In present work we have obtained about 0.8 \AA line widths in the wavelength region 400-800 \AA .

After a wavelength measurement the observed transitions must be assigned to the correct ionization states. The excitation is largely unselective, so that very many levels in several ions of interest can be in the spectra being studied. Many transitions in several ionization degrees appear in a spectrum at certain energy, making the identifications very difficult, and also leading to line-blending in the experimental spectrum. Correct identifications can be achieved by studying the intensity of spectral lines as a function of beam energy, i. e., recording spectra at several energies. This method introduced by [113-114], assumes that the excitation functions for levels within a given ion are similar. We produced and recorded spectra of oxygen in the wavelength region near 500-1500 \AA at beam

energies between 0.6 and 1.7 MeV, to help to identify and correctly assign the observed lines.